

Noise thermometry and electron thermometry of a sample-on-cantilever system below 1 Kelvin

A. C. Bleszynski-Jayich and W. E. Shanks

Department of Physics, Yale University, New Haven, Connecticut 06520, USA

J. G. E. Harris^{a)}

Departments of Physics and Applied Physics, Yale University, New Haven, Connecticut 06520, USA

(Received 17 August 2007; accepted 15 November 2007; published online 9 January 2008)

We have used two types of thermometry to study thermal fluctuations in a microcantilever-based system below 1 K. We measured the temperature of a cantilever's macroscopic degree of freedom (via the Brownian motion of its lowest flexural mode) and its microscopic degrees of freedom (via the electron temperature of a metal sample mounted on the cantilever). We also measured both temperatures' response to a localized heat source. We find that it is possible to maintain thermal equilibrium between these two temperatures and a refrigerator down to at least 300 mK. These results are promising for ongoing experiments to probe quantum effects using micromechanical devices. © 2008 American Institute of Physics. [DOI: 10.1063/1.2821828]

There are at least two distinct “temperatures” relevant to the performance of mechanical devices. The first is the effective temperature associated with the device's Brownian motion. This thermomechanical noise temperature T_n sets a fundamental limit to the device's force sensitivity. It is relevant in magnetic resonance force microscopy (MRFM),^{1,2} atomic force microscopy, and torque magnetometry.^{3–5} It also sets limits on the observation of quantum effects in mechanical oscillators.^{6–9} As a result there is a considerable interest in lowering this “Brownian” temperature via cryogenics^{10–13} and/or cold damping techniques such as laser cooling.^{14–18}

The second important temperature is that of the cantilever's microscopic degrees of freedom. For sample-on-cantilever experiments, this sets the temperature of the sample attached to the cantilever, T_e and is important for MRFM and torque magnetometry experiments.^{3–5,19,20}

In principle, both T_n and T_e can be lowered by placing the cantilever in contact with a thermal bath (i.e., a refrigerator) at temperature T_b . However, thermal equilibrium between the bath, the lever's Brownian motion, and a sample affixed to the lever is not assured. Factors preventing equilibration include the extreme aspect ratio of typical cantilevers, their high quality factors, the insulating nature of most cantilever materials, and the injection of heat by the lever's readout mechanism (e.g., a laser).

Previous experiments have studied T_e of a sample at the end of a gold-coated cantilever between 4 and 16 K.¹⁹ In other experiments, T_n has been cooled in a refrigerator to 200 mK in micromechanical systems¹⁰ and to 56 mK in nanomechanical devices.¹² We are not aware of any direct measurements of both T_n and T_e in a single system.

Here, we present measurements of T_n of a cantilever and T_e of an aluminum grain attached at the end of the cantilever. T_n is measured via the cantilever's Brownian motion, while T_e is measured via the grain's superconducting critical field H_c . We also measure the response of T_n and T_e to the laser interferometer which monitors the cantilever. We find that T_n and T_e remain in good contact with each other and with T_b for temperatures down to 300 mK and laser powers P_{inc} be-

low ~ 150 nW. At higher laser powers, T_e and T_n increase above T_b in a manner consistent with diffusive phonon-mediated heat transport through the cantilever.

These experiments were performed in a ³He refrigerator.²¹ A schematic of the setup is shown in Fig. 1(a). A single crystal silicon cantilever²² of length $L=500$ μm , width $w=100$ μm , thickness $\tau=1$ μm , and doping of $\sim 10^{18}$ cm^{-3} is mounted on a piezoelectric actuator and thermally linked to the refrigerator. A fiber optic interferometer is used to measure the cantilever deflection x . This interferometer is formed between the cantilever and the cleaved face of a single mode optical fiber ~ 100 μm from the cantilever. The interferometer uses a laser wavelength $\lambda=1550$ nm.

The noise temperature is determined by measuring the mean square displacement $\langle x^2 \rangle$ of the cantilever's free end. From the equipartition theorem $T_n = k_0 \langle x^2 \rangle / k_B$, where k_0 is the cantilever's spring constant. To obtain an absolute measurement of the displacement x , we calibrate the interferometer signal by applying a sinusoidal drive to the piezoactuator and measuring the fundamental Fourier component of the interferometer signal on a lock-in amplifier as a function of the drive amplitude. The data are shown in Fig. 2(a).

To fit these data, we note that the optical field at the photodiode has two sources: light reflected from the fiber's end E_1 (which we assume is constant) and light reflected from the cantilever E_2 (we take E_1 and E_2 to be complex). As the cantilever deflects, the phase of E_2 changes, producing

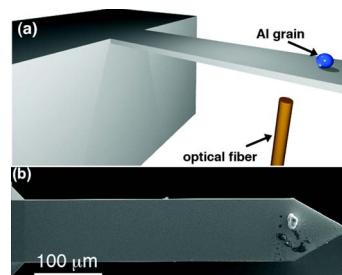


FIG. 1. (Color online) (a) Experimental schematic. Laser interferometry is used to monitor the deflection of a cantilever (shown here with an Al particle attached). (b) SEM image showing an Al grain attached at the end of a Si cantilever. Scale bar is 100 μm .

^{a)}Electronic mail: jack.harris@yale.edu.

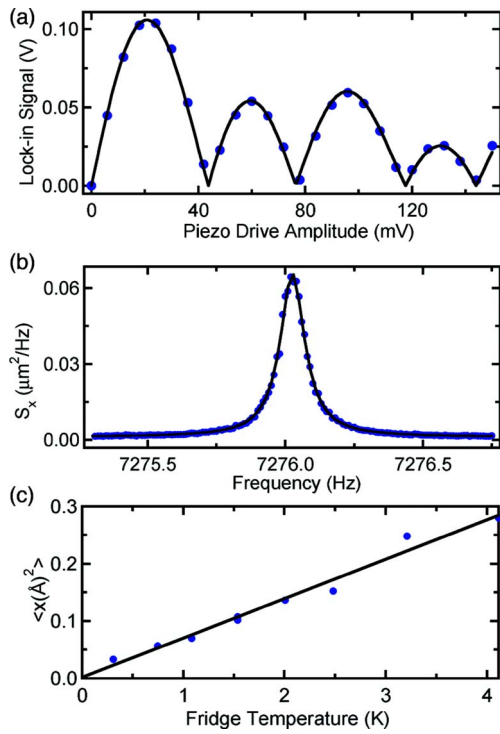


FIG. 2. (Color online) Cantilever noise thermometry. (a) Calibration of the interferometer signal. The plotted points show the lowest Fourier component of the interferometer signal (measured by a lock-in amplifier) as a function of the drive amplitude. The solid line is a fit. (b) The power spectral density of the cantilever's undriven motion at 4.2 K showing the Brownian motion. (c) Mean square displacement of the cantilever as a function of the refrigerator temperature. The linear fit gives a near-zero intercept (solid line), showing the cantilever's undriven motion is thermal.

the interferometric signal. The cantilever deflection also modulates the amplitude of E_2 since the amount of reflected light coupled back into the fiber varies with the cantilever's angle relative to the fiber axis. This effect is small enough to be expanded to first order in x . Thus, we can write the total field at the photodiode as $E_{\text{tot}} = E_1 + E_2^{(0)}(1 + \varepsilon\{x(t) - x_0\})e^{2ikx(t)}$, where $k = 2\pi/\lambda$, $\varepsilon \equiv \partial E_2 / \partial x|_{x=x_0}$, $\varepsilon(x(t) - x_0) \ll 1$, x_0 is the equilibrium position of the cantilever, and $E_2^{(0)}$ is the value of E_2 for $x = x_0$. The time dependent cantilever position is $x(t) = x_0 + x_1 \sin(2\pi ft)$, where x_1 is the amplitude of the cantilever's oscillation and f is its frequency. The lock-in signal $V_{\text{lock-in}}$ is proportional to the Fourier component of $|E_{\text{tot}}|^2$ at f :

$$V_{\text{lock-in}} \propto 2E_2^2 \varepsilon x_1 - 4E_1 E_2 \sin(2kx_0) J_1(2kx_1) + 2E_1 E_2 \varepsilon \cos(2kx_0) x_1 \{J_0(2kx_1) - J_2(2kx_1)\},$$

where J_n is the n^{th} Bessel function of the first kind, and we have kept terms linear in ε . Fitting the data in Fig. 2(a) to this expression allows us to convert $V_{\text{lock-in}}$ to an absolute displacement x in terms of the known laser wavelength.

We then monitor the interferometer signal when no drive is applied to the piezoactuator and use the calibration described above to convert this signal to S_x , the power spectral density of the cantilever's undriven motion [Fig. 2(b)]. The data are fit to the response function of a damped harmonic oscillator, giving a quality factor $Q = 70\,000$ and a resonant frequency $f_0 = 7276$ Hz. The baseline in Fig. 2(b) is a factor of 4 above the photon shot noise. The cantilevers used in the T_n measurements did not have an Al grain attached.

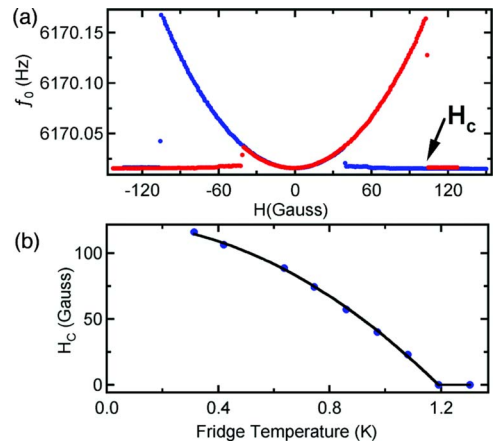


FIG. 3. (Color online) Thermometry of an aluminum grain attached to the end of a cantilever. (a) Cantilever resonant frequency as a function of applied magnetic field at $T_b = 300$ mK. As the field is swept in the positive direction (red curve), an abrupt jump in f_0 occurs at the superconducting critical field $H_c = 110$ G, indicated on the graph. The blue (red) curve is taken during negative (positive) field sweep. (b) Critical field of the Al grain plotted as a function of refrigerator temperature. The blue circles are data and the black curve is a fit to BCS theory.

The area under the fit in Fig. 2(b) (after subtracting the baseline) is $\langle x^2 \rangle$. We measured $\langle x^2 \rangle$ at refrigerator temperatures between $T_b = 300$ mK and 4.2 K [Fig. 2(c)]. The linear dependence of $\langle x^2 \rangle$ on T_b and its extrapolation to zero at $T_b = 0$ K confirm that the force noise driving the cantilever is thermal and, hence, that the motion in Fig. 2(b) is Brownian. Importantly, Fig. 2(c) indicates that T_n remains in equilibrium with the refrigerator down to 300 mK for $P_{\text{inc}} = 150$ nW. The slope of the fit yields $k_0 = 0.02$ N/m, in agreement with the manufacturer's specifications.

To determine the electron temperature of a sample on a cantilever, we measure a nominally identical cantilever on the same chip to which we attached a ~ 10 μm diameter Al grain (99.99% pure).²³ A scanning electron micrograph (SEM) of a cantilever with attached Al grain is shown in Fig. 1(b). We drive the cantilever in a phase-locked loop and measure f_0 as a function of applied magnetic field H , as shown in Fig. 3(a). The red data (positive sweep of H) and blue data (negative sweep) have been shifted slightly to correct for hysteresis in the magnet.

Figure 3(a) shows that below a critical field H_c (indicated on the graph), $f_0 \propto H^2$, while above H_c , f_0 abruptly drops back to its $H = 0$ value and ceases to depend on H . We interpret this jump as the grain's transition from the superconducting state to the normal state. The quadratic dependence of f_0 on H in the superconducting state arises from a combination of the grain's Meissner effect, which induces a magnetic moment $m \propto H$, and the grain's nonspherical shape. This combination causes the grain's energy E to depend on the angle θ its principal axis makes with H . The θ dependence of E results from the energy associated with the grain's demagnetizing fields $E_D = \frac{1}{2} \mu_0 m^2 N(\theta)$, where $N(\theta)$ is a shape anisotropy factor.²⁴ The shift in f_0 is proportional to $\partial^2 E / \partial \theta^2$ which, in turn, is proportional to H^2 . The hysteresis seen in Fig. 3(a) is due to supercooling of the Al particle.²⁵

Figure 3(b) shows H_c as a function of T_b . Fitting the data using Bardeen-Cooper-Schrieffer (BCS) theory²⁶ (which predicts $H_c(T) \approx H_c(0)[1 - (T_e/T_c)^2]$) yields $H_c(0) = 123$ G and $T_c(0) = 1.19$ K. This value of T_c agrees with the value for AlP license or copyright; see <http://apl.aip.org/apl/copyright.jsp>

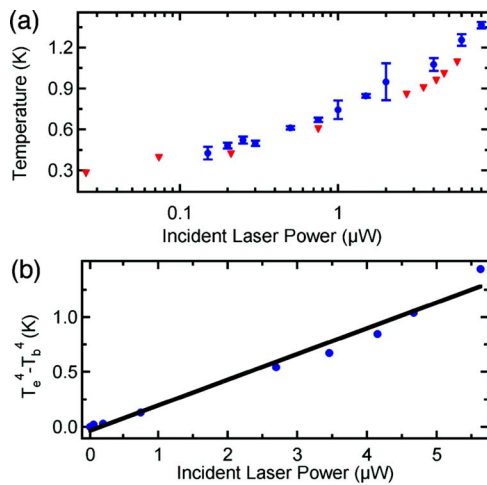


FIG. 4. (Color online) (a) Electron temperature (red triangles) and noise temperature (blue circles) as a function of laser power incident on the cantilever. The refrigerator temperature is 300 mK at the lowest laser power, and increases slightly for the highest laser powers. (b) A phonon thermal conductivity model (solid line) is used to fit the temperature difference between the refrigerator and the aluminum particle (blue dots).

bulk aluminum. The measured $H_c(0)$ is slightly greater than that of the bulk value, which may be due to finite size effects, the grain's nonspherical shape, and the presence of trace impurities.²⁷ The data and fit in Fig. 3(b) indicate that T_e follows T_b down to 300 mK for $P_{\text{inc}}=25$ nW.

The data in Figs. 2(c) and 3(b) confirm that the cantilever's undriven motion and the Al grain's H_c serve as thermometers for T_n and T_e , respectively. We can use these thermometers to measure the response of T_n and T_e to a localized heat source by measuring $\langle x^2 \rangle$ and H_c as a function of P_{inc} . Figure 4(a) shows T_n and T_e versus P_{inc} at $T_b=300$ mK. For the lowest laser powers used, T_n and T_e are equal to T_b , as discussed above. Figure 4(a) shows that higher P_{inc} causes heating of T_n and T_e above T_b , presumably due to partial absorption of the laser by the cantilever.

We model the data in Fig. 4(a) by assuming that the cantilever has a thermal conductivity $\kappa(T)$, a fixed temperature T_b at its base, and a heat source $\dot{Q}=\alpha\tau P_{\text{inc}}$ at the location of the laser spot, where α is the cantilever's optical absorption coefficient. At the temperatures of our experiment heat transport in the cantilever is dominated by phonons, so we expect $\kappa(T)=bT^3$, where b is a constant. This gives $\dot{Q}=w\tau b/4L^*(T_e^4-T_b^4)$, where $L^*=400$ μm is the distance between the laser spot and the cantilever base. In Fig. 4(b), we plot the measured $T_e^4-T_b^4$ as a function of P_{inc} . The solid line is a fit to the expression above.

Assuming a typical value of $b=0.07$ W/m K (Refs. 4 and 28) gives $\alpha=10$ cm^{-1} . This result for α agrees with direct measurements of optical loss in similarly doped Si at cryogenic temperatures.²⁹ We note that measurements of optical loss typically compare incident optical power with transmitted and reflected power, and so measure the sum of absorption and diffusive scattering. Our result for α is a direct measurement of absorption.

Previous experiments found higher T_n for a given P_{inc} than in Fig. 4.¹⁰ This may be due to the differences in the cantilevers used; those studied here are 25 times wider and three times thicker than those in Ref. 10. This should lead to

higher thermal conductance (and hence lower T_n) in our levers as a result of geometric considerations and decreased phonon boundary scattering.³⁰ These effects seem to offset the larger optical absorption of our cantilevers, which is presumably due to the higher doping density.²⁹

In conclusion, we have measured both the thermomechanical noise temperature and the sample temperature for a sample-on-cantilever system. Both can remain in thermal contact with a bath for temperatures at least as low as 300 mK. Given the signal-to-noise ratio in Fig. 2(b), this approach could be used with much smaller samples, including microfabricated devices. We also determined the optical absorption of the cantilever.

We acknowledge discussions with Michel Devoret.

- ¹J. A. Sidles, J. L. Garbini, K. J. Bruland, D. Rugar, O. Zuger, S. Hoen, and C. S. Yannoni, *Rev. Mod. Phys.* **67**, 249 (1995).
- ²D. Rugar, R. Budakian, H. J. Mamin, and B. Chui, *Nature (London)* **430**, 329 (2004).
- ³J. G. E. Harris, D. D. Awschalom, R. Knobel, N. Samarth, K. D. Maranowski, and A. C. Gossard, *Phys. Rev. Lett.* **86**, 4644 (2001); J. G. E. Harris, R. Knobel, K. D. Maranowski, A. C. Gossard, N. Samarth, and D. D. Awschalom, *Appl. Phys. Lett.* **82**, 3532 (2003).
- ⁴Y. Wang, L. Li, M. J. Naughton, G. D. Gu, S. Uchida, and N. P. Ong, *Phys. Rev. Lett.* **95**, 247002 (2005).
- ⁵M. P. Schwarz, D. Grundler, I. Meinel, C. H. Heyn, and D. Heitmann, *Appl. Phys. Lett.* **76**, 3564 (2000).
- ⁶W. Marshall, C. Simon, R. Penrose, and D. Bouwmeester, *Phys. Rev. Lett.* **91**, 130401 (2003).
- ⁷A. Ferreira, A. Geirreiro, and V. Vedral, *Phys. Rev. Lett.* **96**, 060407 (2006).
- ⁸M. Pinar, A. Dantan, D. Vitali, A. Arcizet, T. Briant, and A. Heidman, *Europhys. Lett.* **72**, 747 (2005).
- ⁹V. Braginsky and S. P. Vyatchanin, *Phys. Lett. A* **293**, 228 (2002).
- ¹⁰H. J. Mamin and D. Rugar, *Appl. Phys. Lett.* **79**, 3358 (2001).
- ¹¹S. Groblacher, S. Gigan, H. R. Böhm, and A. Zeilinger, e-print arXiv:quant-ph/0705.1149.
- ¹²M. D. LaHaye, O. Buu, B. Camarota, and K. Schwab, *Science* **304**, 74 (2004).
- ¹³A. Naik, O. Buu, M. D. LaHaye, A. D. Armour, A. A. Clerk, M. P. Blencowe, and K. C. Schwab, *Science* **443**, 193 (2006).
- ¹⁴C. H. Metzger and K. Karrai, *Nature (London)* **432**, 1002 (2004).
- ¹⁵S. Gigan, H. R. Böhm, M. Paternostro, F. Blaser, G. Langer, J. B. Hertzberg, K. C. Schwab, D. Bäuerle, M. Aspelmeyer, and A. Zeilinger, *Nature (London)* **444**, 67 (2006).
- ¹⁶D. Kleckner and D. Bouwmeester, *Nature (London)* **444**, 75 (2006).
- ¹⁷O. Arcizet, P.-F. Cohadon, T. Briant, M. Pinar, and A. Heidmann, *Nature (London)* **444**, 71 (2006).
- ¹⁸J. D. Thompson, B. M. Zwickl, A. M. Jayich, Florian Marquardt, S. M. Girvin, and J. G. E. Harris, e-print arXiv:quant-ph/0707.1724.
- ¹⁹K. R. Thurber, L. E. Harrell, and D. D. Smith, *J. Appl. Phys.* **93**, 4297 (2003).
- ²⁰H. J. Mamin, M. Poggio, C. L. Degen, and D. Rugar, *Nat. Nanotechnol.* **2**, 301 (2007).
- ²¹Janis Research, Wilmington, MA, USA.
- ²²NanoWorld, Neuchâtel, Switzerland.
- ²³ESPI Metals, Ashland, OR, USA.
- ²⁴E. C. Stoner and E. P. Wohlfarth, *Philos. Trans. R. Soc. London, Ser. A* **240**, 599 (1948).
- ²⁵T. E. Faber, *Proc. R. Soc. London, Ser. A* **231**, 353 (1955).
- ²⁶J. Bardeen, L. N. Cooper, and J. R. Schrieffer, *Phys. Rev.* **108**, 1175 (1957).
- ²⁷M. H. Devoret (private communication).
- ²⁸M. Ashghi, K. Kurabayashi, R. Kasnavi, and K. E. Goodson, *J. Appl. Phys.* **91**, 5079 (2002).
- ²⁹P. E. Schmid, *Phys. Rev. B* **23**, 5531 (1981).
- ³⁰M. Ashghi, Y. K. Leung, S. S. Wong, and K. E. Goodson, *Appl. Phys. Lett.* **71**, 1798 (1997).